Segmentation of fractal objects : application to the measure of algae deposit density in the 'green tide' phenomenon

Claude Cariou and Kacem Chehdi

ENSSAT - LASTI Groupe Image
6, rue de Kerampont - BP 447
22305 Lannion Cedex - France
Tel: (+33) (0)2-96-46-50-30; Fax: (+33) (0)2.96.46.66.75
e-mail: Claude.Cariou@enssat.fr, Kacem.Chehdi@enssat.fr

ABSTRACT

In this communication, we present an original unsupervised image segmentation procedure which assumes the 2-D objects to be fractal. This technique is applied to the evaluation of the covering rate of algae deposit in the 'green tide' phenomenon which occurs on the coasts of Brittany. After a discussion relative to the fractal nature of the objects under study, we introduce a fractal growth model called DLA which, in conjunction with the image data, allows the obtention of a binarized image. For this, a Bayesian formulation is adopted. Some experimental results are presented, which show the potentiality of this approach.

1 Introduction

The so-called 'green tide' phenomenon is characterized by the proliferation of green algae (*ulvea*) within bays with typical closed topology, which are numerous around the Breton coasts. Under certain conditions of sea current and swell, this phenomenon provoques the deposit upon the beach of an equivalent mass of several hundred tons of this kind of algae. The on-site measure of this biomass as an indicator of the nitrate pollution in ground basins is made difficult because the sampling of such surfaces (which may attain 10 km^2) can only be parcimonious, and also because heavy means are necessary.

Aerial imagery can then be of great help for this purpose, because it offers the possibility of acquiring in a single image the whole site under study. However, aerial images do not allow the access to details (which are often very fine) of the deposit under the ground resolution of the sensor (typically 1 m^2). Figure 1 shows an example of such an aerial image.

In this study, we started from the fact that aerial images of the algae deposit are very similar to other images issued from some particular physical process (Diffusion Limited Aggregation - DLA, Dielectric Breakdown Model - DBM) [7] [1]. After several *in situ* analysis which seem to corroborate this fact, we thus conjectured the *fractal* nature of the algae deposit [2], which is thus seen as an objet with a mass dimension less than 2. More precisely, the object that we qualify as fractal is not the algae deposit itself, but the set of channels and micro-channels through which flows the residual sea water, after the deposit of a homogeneous mass of wet algae.

Figure 1: Aerial image of green algae phenomenon (Bay of Lannion – France).

In Figures 2 and 3, we present an example image of a close area with typical deposit, together with a blind binarization (without any prior information), which gives to the reader an idea of the (supposed fractal) object from which the mass dimension should be estimated.

Let us recall here that, for an object with a mass fractal dimension $\triangle$ ($1 \leq \triangle \leq 2$), the mass $M(r)$ within a disc of radius r varies as follows [5] :

$$M(r) \propto r^{\triangle} \qquad (1)$$

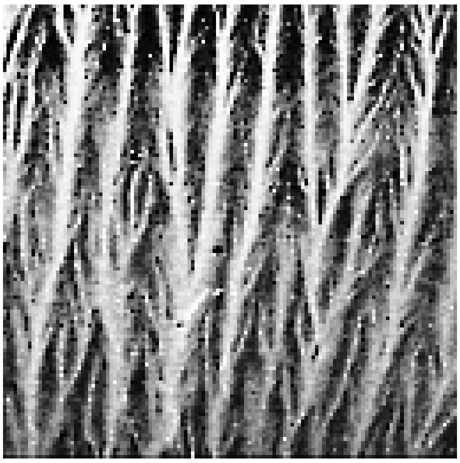

Figure 2: Close view of a fractal algae deposit (128 × 128).

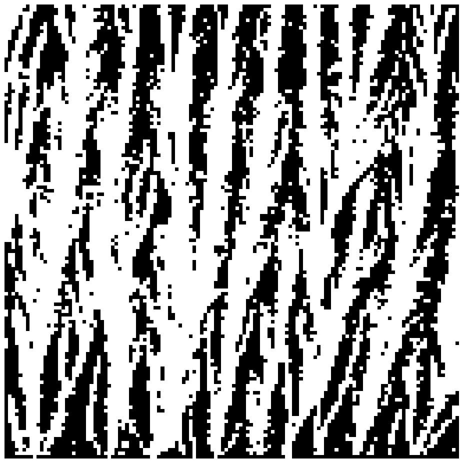

Figure 3: Corresponding blind binarization.

2 In situ measurements

In order to assess the fractal nature of the deposit, we performed several in situ measurements relative to the local covering rate of the green algae which is homogeneous with the mass of our (supposed) fractal object. Finding an experimental methodology for measuring the mass fractal dimension of such an object is quite difficult, because :

• The surfaces under study show long distance related phenomena, as much as 15 up to 25 meters.

• The micro-local (in a range of a few centimeters) algae deposit is subject to a high variability in the decision about the absence or the presence of green algae. Note here that the green algae is made of thin foils of size about 20 centimeter^2.

The mass of the object under study being homogeneous to a surface and more precisely the complementary of the algae deposit surface, one methodology for in situ measurements could be to count and sum the local surface deposit at a sufficient low scale : this technique clearly relates to the so-called 'mass radius' method. However, this approach would be very time-consuming and should be avoided.

Another way of estimating the mass fractal dimension Δ is the cumulative intersection method [3] [4]. It simply consists in choosing at random a central point within the fractal object and counting, for regularly spaced radii $r(i), 0 \leq i \leq N$, the following quantity :

$$CI(i) = \sum_{i=0}^{N-1} I(r(i)) \quad , \tag{2}$$

where N is the number of circles around the central point and $I(r(i))$ is the number of intersections between the object and its background support. Then it is shown that Δ can be estimated as the slope of $\ln(CI(i))$ as a function of $\ln(r(i))$.

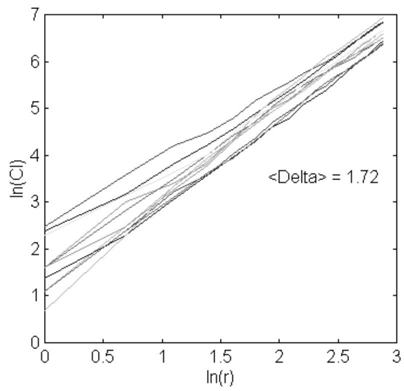

Figure 4: Mass fractal dimension estimation.

In practice, cumulative intersections were measured in situ (with circle radii spaced of 1 m, and $r_{\max} = 20$ m) during two campaigns in summer 1997 and summer 1998, and a rough estimate of $\Delta = 1.72$ was obtained (see Figure 4 for a log-log plot of 11 curves). Thus it appears that the object under study has a mass fractal dimension less than 2, which corroborates the fractal hypothesis. Also, it can be highlighted that this particular value of 1.72 is very close to the theoretical value of the fractal dimension of the DLA process, which is $\Delta_{DLA} = 1.71$.

3 Model-based binarization of a fractal object

3.1 Context and theoretical background

Now that we have assessed the fractal nature of the sea water channels and micro-channels – at least within a certain range –, the question arises about the obtention of a robust *binarization* of such an object with respect to its background, provided the available data is an aerial image of the algae deposit. In this application, despite the fact that color images were available, we have chosen

to work with gray scale images for the sake of simplicity. The main idea of this work relies on a Bayesian framework for a particular DLA process over the square lattice. DLAs have been studied for a least two decades by statisticians and physicists and many theoretical results are available in the literature, with applications in fluid mechanics and dendritic growth [7].
Concerning the simulation of DLA processes, two main approaches exist, namely the random walk on the lattice (also known as the 'drunk ant' approach) [8], and the approach based on solving the Laplace equation [1].
However, both approach seem to be rarely used in an anisotropic context as is the case herein. As a matter of fact, the displacement of the residual sea water during the algae deposit may be locally considered as unidirectional, from the top to the bottom of the beach.
In this work, we finally chose to use the Laplace equation approach, while imposing a particular topology to the problem. The aim of our binarization technique will then be to perform an aggregation of 'particles' which takes into account the probability of aggregation of such a particle to the aggregate (say the fractal object), conditioned to the given image data.

3.2 The proposed technique

Strongly related to the DLA process is the Laplacian growth model. More precisely, considering that the whole aggregate is set at a 'potential' $P = 0$, and the external boundary is set at $P = 1$, this model assumes that the probability of aggregation of a new particle is proportional to the local potential P, which follows the Laplace equation [1] :

$$\nabla P^2 = 0 \tag{3}$$

Upon the square lattice, the preceding equation becomes :

$$P(s) = \frac{1}{M} \sum_t P(s+t) \quad , \tag{4}$$

where the sum holds over the M nearest neighbouring sites $s + t$. In our experiments, we chose $M = 8$. Thus a direct access to the probability of aggregation of a new particle to the aggregate is available at each step through a simple filtering of a potential map $P(s)$.

3.3 Description of the algorithm

We now describe the algorithm used for the binarization of the fractal structure.
The basic idea is to adopt a Bayesian framework that jointly takes into account the DLA model and the fitting to the image data. More precisely, if we call D the DLA aggregate and $y(s)$ the gray level at site s, then the probability of aggregation conditioned to the image data follows :

$$P(s \in D|Y(s))\ f(Y(s)) = f(Y(s)|s \in D)\ P(s \in D) \tag{5}$$

where $f(Y(s))$ is the probability density function of the random variable $Y(s)$. Thus we can write :

$$P(s \in D|Y(s) = y_0) \propto f(Y(s) = y_0|s \in D)\ P(s \in D) \tag{6}$$

Concerning the fitting to image data, one has to impose a 'reasonable' model for $f(Y(s) = y_0|s \in D)$. In this work, we chose the following one :

$$f(Y(s) = y_0|s \in D) \propto \exp(-\beta(y_{\max} - y_0)) \tag{7}$$

Note that other models can probably be adopted, but this question remains beyond the scope of this study.
On the other hand, the probability $P(s \in D)$ is explicitly given by Eq. (4), provided we restrict the site s to the external limit D^+ of the DLA. However, the computation of local potentials requires an updating after each aggregation of a new pixel to the current DLA. This updating can be performed in an iterative manner by applying an isotropic filtering of the potential map P with the following 2-D filter :

$$h = \frac{1}{8} \begin{bmatrix} 1 & 1 & 1 \\ 1 & 0 & 1 \\ 1 & 1 & 1 \end{bmatrix} , \tag{8}$$

until convergence of the resulting map.
Once the new potential map is available, one computes the probability distribution of aggregation at the border of the DLA using Eq. (6). Finally, one performs a random trial according to this distribution and then aggregates the corresponding pixel to the DLA.
To summarize, we give below the general scheme of our technique :

1. *Initialization* : Definition of potential limits $P = 0$ on the DLA and $P = 1$ on the external (far) border. Note that in our experiments, the DLA was chosen to grow from the bottom of the image to the top, and that the only available information for starting the aggregation was the image data.

2. *Laplace equation* : The potential map between the DLA and the external border is computed iteratively as explained above. Without detailing the procedure, image border effects have been taken into account in this step.

3. *Probability computation* : $\forall s \in D^+$, compute the distribution $P(s \in D|Y(s) = y_0)$ according to Eq. (6).

4. *Random trial* : choose at random a site s^* following this distribution.

5. *Aggregation* : let $D \leftarrow D \cup s^*$

6. Return to step 2.

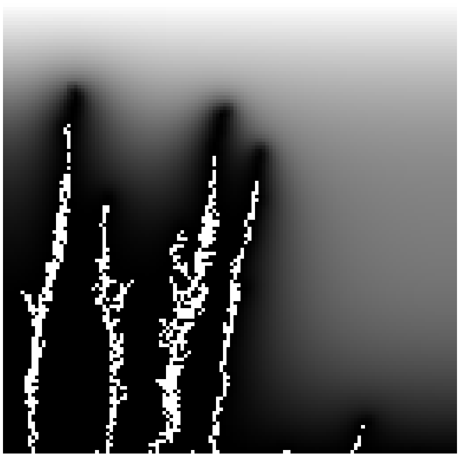

Figure 5: Corresponding potential map.

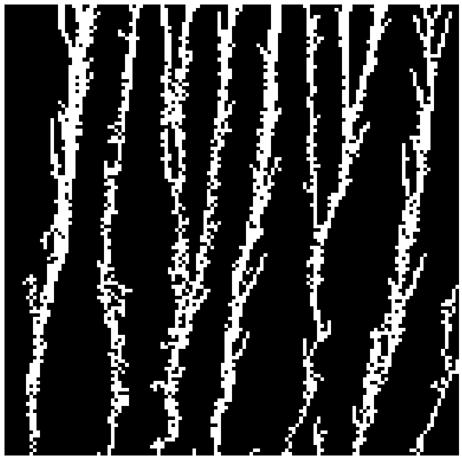

Figure 6: Final binarization.

4 Experimental Results

We now present a sample result of this procedure to the image given in Figure 2. Firstly, an intermediate result of aggregation is presented together with the corresponding current potential map $P(s)$ in Figure 5. On the former, one can see that privileged channels are correctly – while partially – binarized, and that the main branching of the DLA is easily tracked. On the latter, one can see the potential distribution map, which indeed resembles the magnitude of an electric potential field. This also explains why the DLA model is closely related to the Dielectric Breakdown Model (DBM). Note that this results corresponds to an aggregation of 1000 pixels.

Figure 6 presents the final binarization of the image, that can be compared to Figure 3. Here the fractal growth required the aggregation of 3000 pixels. One can remark the quality of the binarization in comparison with the blind one, although some branched structures at the bottom of the image are missing.

5 Conclusion

In this communication, we have presented an original segmentation (binarization) procedure which takes into account the fractal nature of the objects under study. This techniques associates to the image data an *a priori* model of structure growth, called DLA, which helps the segmentation process. This model and the given image data are combined within a Bayesian framework. While the results presented are quite preliminary, we hope that a refinement of the aggregation model and a better modeling of the underlying physics with the image data can produce even better results. To finish with, let us point out that the approach presented herein has many similarities with a technique developed in 3-D medical imagery [6] for the retrieval of arterial structures.

6 Acknowledgements

Authors would like to express their thanks to Prof. Alain Le Méhauté (Université de Nantes) for fruitful discussions about 2-D fractal objects, to Mr. Pascal Talec (formerly CEVA - Pleubian) for the providing of aerial images and to Dr. Christophe Rosenberger (ENSI de Bourges) for his help in measurements campaigns.

References

[1] A. Aharony, "Fractal growth," in *Fractals and Disordered Systems*, A. Bunde, S. Havlin (Eds.), Springer-Verlag, Berlin, 1991.

[2] C. Cariou, "Segmentation d'objets fractals: application à la mesure de densité de dépôt d'algues dans le phénomène de marée verte," communication orale au GT2 – OT2.2: Fractales et Ondelettes, GdR-PRC ISIS, mars 2000.

[3] H.F. Jelinek and E. Fernandez, "Neurons and fractals: how reliable and useful are calculations of fractal dimensions ?," J. Neurosci. Meth. **81**, pp. 9–18, 1998.

[4] H.F. Jelinek, FractopV02, http://life.csu.edu.au/fractop

[5] A. Le Méhauté, *Les Géométries Fractales*, Traité des Nouvelles Technologies, Hermes, Paris, 1990.

[6] H.-O. Peitgen et al., "Mathematik, Complexe Systeme, Medizin : von der Potentialtheorie zu neuen radiologischen Werkzeugen," in *Visualisierung in Mathematik, Technik und Kunst. Grundlagen und Anwendungen*, A. Dress, G. Jaeger (Eds.), Vieweg und Sohn, Verlagsgesellschaft, pp. 91–107, 1999.

[7] H.E. Stanley, "Fractals and multifractals: the interplay of physics and geometry," in *Fractals and Disordered Systems*, A. Bunde, S. Havlin (Eds.), Springer-Verlag, Berlin, 1991.

[8] T.A. Witten and L.M. Sander, *Phys. Rev. Letters*, **47**, pp. 1400–*ff*, 1981.